Available online at www.sciencedirect.com
SCIENCE DIRECT®
ELSEVIER
International Journal of Mass Spectrometry 228 (2003) 359–371
International Journal of Mass Spectrometry
www.elsevier.com/locate/ijms

Specific reactivity of 1-alkenes with transition metal cations 1-Pentene– and 1-octene–Cu^+ reactions in the gas phase

A. Luna[a], O. Mó[a], M. Yáñez[a,*], J.-P. Morizur[b], E. Leclerc[b], B. Desmazières[b], V. Haldys[b], J. Chamot-Rooke[b,1], J. Tortajada[b]

[a] *Departamento de Química, C-9, Universidad Autónoma de Madrid, Cantoblanco, 28049 Madrid, Spain*
[b] *Laboratoire Analyse et Environnement, UMR CNRS 8587, Université d'Evry Val d'Essonne, Bâtiment des Sciences, Boulevard François Mitterrand, 91025 Evry Cedex, France*

Received 7 November 2002; accepted 18 March 2003

This paper is dedicated to Prof. Helmut Schwarz on the occasion of his 60th birthday.

Abstract

The topology of the potential energy surface associated with 1-pentene–Cu^+ and 1-octene–Cu^+ was investigated through the use of high-level density functional theory calculations. This theoretical survey, together with a combination of tandem mass spectrometry and isotopic labeling experiments carried out for 1-octene, confirm that the pseudo-insertion mechanism tentatively proposed by Fordham et al. [J. Mass Spectrom. 34 (1999) 1007], is the most favorable one. In this mechanism, attachment of the metal cation to the π-system forces a folding of the alkyl chain which favors the formation of an hexa-coordinated intermediate much more stable than the complexes formed along a typical dissociative attachment process. We have also shown that the main features of the pseudo-insertion mechanism do not change when the alkyl chain attached to the C=C double bond is much longer. Hence, we can safely conclude from our calculations and the experimental results obtained for 1-octene deuterated derivatives, that this mechanism would explain, in general, the specific reactivity of Cu^+ with alkenes. We have also shown that the minor loss of H_2 systematically observed in these gas-phase processes, would be related with the ability of Cu^+ to yield strong agostic interactions either with the methylene groups or with the terminal methyl group of the alkyl chain.

Keywords: Specific reactivity; 1-Alkenes; Transition metal; Cations; Density functional theory calculations

1. Introduction

The study of gas-phase reactions involving transition metal cations, through the use of different mass spectrometry techniques, had a great impact in our knowledge on the bonding of many molecular species of interest in different fields of modern chemistry and biochemistry. At the same time a better knowledge on the intrinsic behavior of many compounds with respect to transition metal cations was achieved [1–3]. As a consequence, the intimate mechanisms of many processes in catalysis, molecular recognition, biochemistry, analytical, organometallic and environmental chemistry were established [4–6]. Many

* Corresponding author. Tel.: +34-9139-749-53; fax: +34-9139-752-38.
E-mail address: manuel.yanez@uam.es (M. Yáñez).
[1] Permanent address: Département de Chimie, Laboratoire des Mechanismes Réactionnels, UMR CNRS 7651, Ecole Polytechnique, 91128 Palaiseau Cedex, France.

1387-3806/$ – see front matter © 2003 Elsevier Science B.V. All rights reserved.
doi:10.1016/S1387-3806(03)00130-1

of these achievements were possible because of the availability of powerful computational schemes based on the use of the molecular orbital or density functional theories [7–11]. Indeed, the mechanisms of reactions involving transition metal cations are usually quite complicated, because many states, close in energy, are accessible. Hence, only an accurate description of the topology of the corresponding potential energy surface (PES), in conjunction with the experimental evidence, permit to elucidate unambiguously the most favorable reaction paths. Schwarz and coworkers [12–14] made outstanding contributions in this area, and the so-called two-state reactivity is a good example of the aforementioned fruitful interplay between theory and experiment.

Another common characteristic of reactions involving transition metal cations, whose understanding requires a precise knowledge of the characteristics of the PES, is their specificity, which besides, is very important from the analytical point of view [15–19]. In this respect, the analysis of alkenes represents an interesting example because, this analysis is a challenge when mass spectrometry based on electron ionization (EI) is used, because the loss of structural information produced under impact ionization conditions prevents the localization of the double bond. Conversely, cationization of the alkene by transition metal cations does not only yields the molecular mass information but provides also rich fragmentation patterns, from which it is possible to extract useful structural information. Some examples based on the use of Fe^+ can be found in the literature [20–26] and some insertion mechanisms were proposed. The work of Peake and Gross [27] and that of Armentrout et al. [28] showed that Cu^+ and Co^+ can also activate allylic bonds. Also in this area, Schwarz [29] has made significant contributions.

In a recent paper, Fordham et al. [19] showed, through the use of new chemical ionization (CI)/fast atom bombardment (FAB) techniques that gas phase reactions of different alkenes with Cu^+ permit identifying the position of the double bonds and the differentiation of the alkene isomers. In the same paper, possible mechanisms for the different unimolecular decompositions were tentatively proposed. The aim of this paper is to investigate, through the use of high level density functional theory (DFT) methods, the topology of the potential energy surface associated with some alkene–Cu^+ reactions, in order to assess the reliability of those mechanisms and to provide a quantitative description of them compatible with the preliminary experimental results [19]. We shall show, by means of high-level DFT calculations, and by a combination of tandem mass spectrometry and isotopic labeling experiments, taking 1-pentene and 1-octene as suitable model systems, that the mechanisms proposed are indeed general, and therefore, applicable not only to 1-pentene but to larger 1-alkenes, irrespective of the length of the alkyl chain attached to the unsaturated group.

2. Experimental

2.1. Instrumentation

Experiments were conducted using a ZAB-HSQ (VG Analytical) hybrid mass spectrometer of BEqQ configuration, a reverse-geometry instrument which allows the acquisition of mass-analyzed ion kinetic energy (MIKE) spectra.

Metal-ion complexes were formed in situ using a CI/FAB ion source, first described by Freas et al [30]. Copper ions were generated by bombarding a copper wire target with xenon atoms emitted by a FAB gun (7 keV kinetic energy, 1.2 mA emission current). 1-Octene and its isotopologues were introduced via an HP5970A gas chromatograph fitted with an apolar capillary column (J.W. DB5 MS, 30 m × 0.24 mm i.d., film thickness 0.25 μm). The latter was passed directly into the CI/FAB source of the mass spectrometer. The short length (∼20 cm) of column between the oven of the gas chromatograph and the source inlet (transfer line) was encased in a length of insulated copper tubing. Nitrogen was used as the carrier gas (head pressure 80 kPa), flow-rate 1 mL min^{-1}. Samples (2 μL of a 1‰ (v/v) solution diluted in pentane were injected in the splitless mode. For analysis the column was held at 60 °C and the pseudomolecular ions of copper ^{65}Cu

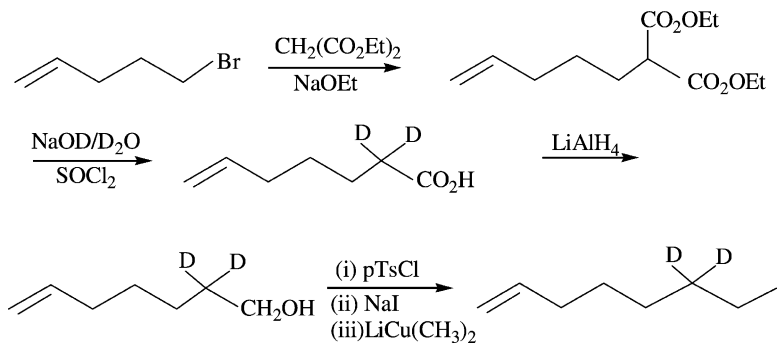

Scheme 1.

adducts of the 1-octene and or its isotopologues was selected as the parent ion and the electric sector of the mass spectrometer was scanned over the range of 4000–8000 V at a rate of 1 s^{-1}.

2.2. Chemicals

1-Octene and copper wire were purchased from Aldrich. 1,1-d_2-1-Octene was obtained from Cambridge Isotope Laboratories. The 8,8,8-d_3-1-octene, the 7,7-d_2-1-octene and the 6,6-d_2-1-octene were synthesized by standard laboratory procedures previously described [31,32]. For example, the 6,6-d_2-1-octene was prepared according to the route depicted in Scheme 1 starting from 5-bromo-1-pentene (Aldrich). The synthesis was achieved by (a) nucleophilic displacement with diethyl malonate, (b) saponification of the resulting diester with sodium deuteroxide, (c) decarboxylation of the diacid, (d) reduction of the carboxylic acid by $LiAlH_4$, (e) iodination of the resulting alcohol via a tosylate derivative, and (f) cross-coupling reaction of the resulting iodide by the lithium dimethyl cuprate. 6-Bromo hexene (Aldrich) was used as starting material for the synthesis of the 8,8,8-d_3-1-octene and the 7,7-d_2-1-octene.

3. Computational details

The geometries, harmonic vibrational frequencies and final energies of the different species under consideration were optimized by using the hybrid B3LYP functional, as implemented in the Gaussian-98 suite of programs [33].

This DFT approach combines the Becke's three-parameter non-local hybrid exchange potential [34] with the non-local correlation functional of Lee et al. [35]. For geometry optimizations, we have used the all electron (14s9p5d/9s5p3d) basis of Watchers-Hay, supplemented with one set of f polarization functions for Cu [36,37] and the 6-311G(d,p) basis set for the remaining atoms of the system. The harmonic vibrational frequencies of the different stationary points of the PES have been calculated at the same level of theory in order to classify them as local minima or transition states (TS), and to estimate the corresponding zero point energies (ZPE). In general, both geometries and vibrational frequencies obtained using this approach are in fairly good agreement with experimental values [38,39]. In general, the compounds investigated present a large number of conformers corresponding to different arrangements of the alkyl chain. In what follows, we shall refer exclusively to the most stable one.

Final energies were obtained by using an enlarged basis set, in which the standard 6-311+G(2df,2p) basis set for first row-atoms was combined with a (14s9p5d/9s5p3d) Watchers-Hay's basis, supplemented with a set of (1s2p1d) diffuse components and with two sets of *f* functions and one set of *g* functions as polarization basis for Cu. It has been shown [40,41] for some smaller Cu^+ complexes that the

binding energies so obtained are quite reliable. Also importantly, the B3LYP approach was found to be superior than typical high level ab initio formalisms, such as the G2 theory, as far as the description of Cu^+ complexes is concerned [40,42].

The electronic structure of the systems under study was analyzed by means of the atoms in molecules (AIM) theory [43], which is based in a topological analysis of the electron density function, $\rho(r)$ and by means of the natural bond orbital (NBO) analysis. Using the AIM approach we have located the relevant bond critical points (bcps), whose charge density is a good index of the strength of the linkage. The AIM analysis was performed using the AIMPAC series of programs [44]. The NBO method [45], through a second-order perturbation analysis, provides useful information on the interaction between the alkene and the metal cation, in terms of dative bonds from occupied orbitals of the former toward vacant orbitals of Cu^+, and back-donation from occupied orbitals of Cu^+ toward antibonding orbitals of the alkene. The NBO analysis has been carried out with the NBO program package [46].

4. Results and discussion

In general, as shown in [19], the MIKE spectra of the alkene–Cu^+ complexes show a single intense fragmentation accompanied by much less intense fragments. For example, the principal fragmentations observed for 1-pentene–Cu^+ correspond to losses of C_2H_4 (100), C_3H_6 (16) and H_2 (8). For 1-octene the product distribution is C_3H_6 (100), C_5H_{10} (6) and H_2 (5). Also importantly, the reactions with Fe^+, Ni^+ and Co^+ lead to the same products. For these latter cases, a mechanism of insertion into a C–C allylic bond leading to an $[(alkene)_2–Fe]^+$ complex, which decomposes revealing the double bond position, was proposed [21]. However, since different from the aforementioned transition metal cations, Cu^+ presents a complete d^{10} shell, and therefore, is formally a closed-shell system, a different dissociative attachment mechanism was usually assumed [27].

In our theoretical study, we have explored, for the olefin loss, these two possibilities for 1-pentene and 1-octene as well as the possible mechanisms involved in the observed minor loss of H_2 only in the case of 1-pentene. It is reasonable to assume that the starting point for both mechanisms would be the formation of a conventional π-complex (**1**). From complex **1**, the dissociative attachment mechanism **I** would involve, as a first step, the transfer of the γ-hydrogen toward Cu^+ to yield structure **2** (see Fig. 1). A subsequent transfer of this hydrogen to the α-carbon would lead directly the dissociation products, namely $C_2H_3R + [C_3H_6Cu]^+$ (**P1**). The second possible mechanism **II** corresponds to a pseudo-insertion process, in which the metal cation does not insert, strictly speaking, into the C–C bond but interacts with the two moieties produced upon the C3–C4 bond fission to yield a hexa-coordinated structure **3**. Complex **3** will eventually evolve, through the transition state **TS34**, to yield complex **4**. The dissociation of **4** would lead either to the loss of C_2H_3R (**P1**) or to the loss of C_3H_6 (**P2**). Mechanism **III** is associated with the observed loss of H_2 and involves agostic interactions of Cu^+ with α and γ CH bonds.

4.1. 1-Pentene–Cu^+ reactions

4.1.1. Olefin loss

The optimized structures of 1-pentene and those of the different local minima involved in mechanisms **I–III** have been schematized in Fig. 2. This figure contains also the optimized geometries of the different products. The geometries of the transition states have not been included in this figure for the sake of conciseness, but they are available from the authors upon request. The total energies of all the stationary points associated with the three mechanisms investigated have been summarized in Table 1. For a better comparison, the relative energies included in Fig. 1 refer to the entrance channel. The first conspicuous fact from Fig. 1 is that dissociative attachment mechanism **I** is thermodynamically disfavored because structure **2** lies almost 17 kcal mol^{-1} above the reactants. Conversely, the pseudo-insertion mechanism **II**

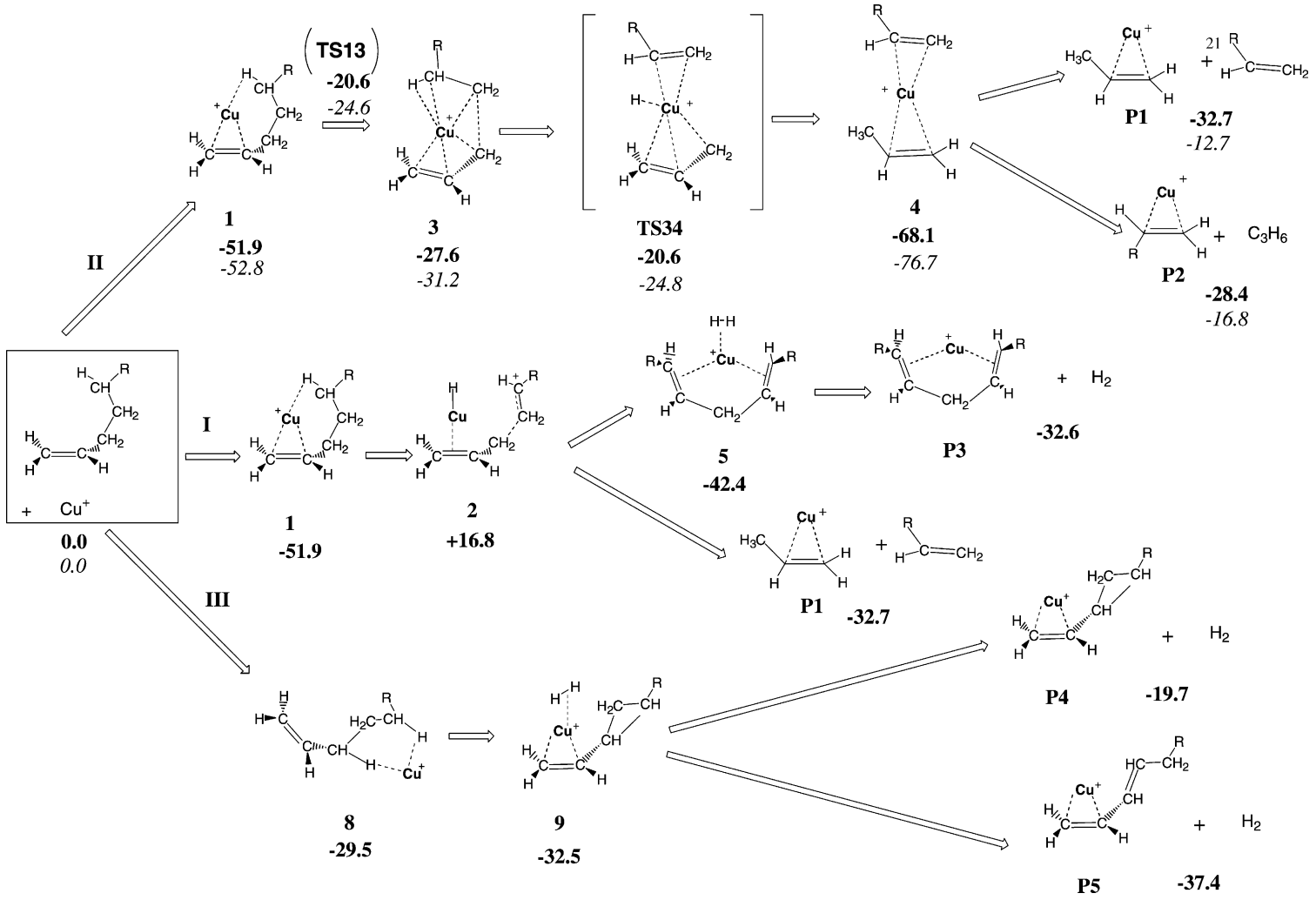

Fig. 1. Schematic representation of the possible mechanisms involved in the unimolecular fragmentation of 1-pentene–Cu^+ (R = H) and 1-octene–Cu^+ (R = C_3H_6) complexes in the gas phase. Relative energies (kcal mol^{-1}), have been referred to the energy of the corresponding entrance channel. Numbers in bold correspond to 1-pentene–Cu^+ reactions and numbers in italic correspond to 1-octene–Cu^+ reaction.

is thermodynamically possible, since the whole PES lies lower in energy than the reactants.

To understand these differences and, although a detailed discussion of the structures of 1-pentene–Cu^+ complexes is not the aim of our paper, some features should be singled out for comment, because they will permit a better understanding of the changes observed in the relative stability of the different stationary points of the PES. The first important feature is that the most stable 1-pentene–Cu^+ adduct corresponds to a structure (**1**) in which the alkyl chain coils up to enhance its interaction with the metal cation. The stability of this coiled structure is important because it will favor the pseudo-insertion mechanism, that would not

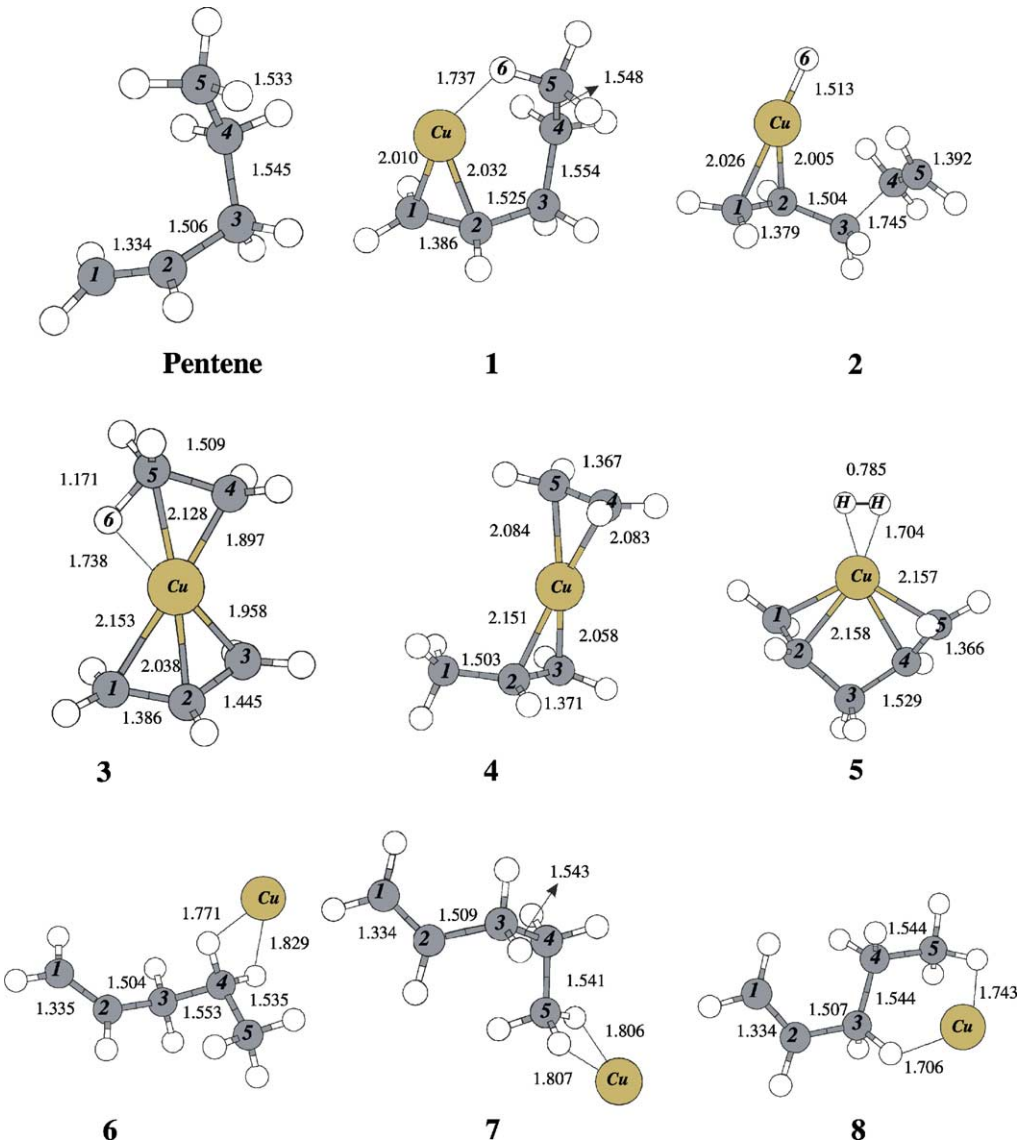

Fig. 2. Optimized geometries of the relevant local minima of 1-pentene–Cu^+ and 1-octene–Cu^+ potential energy surfaces. Bond lengths in angstrom (Å).

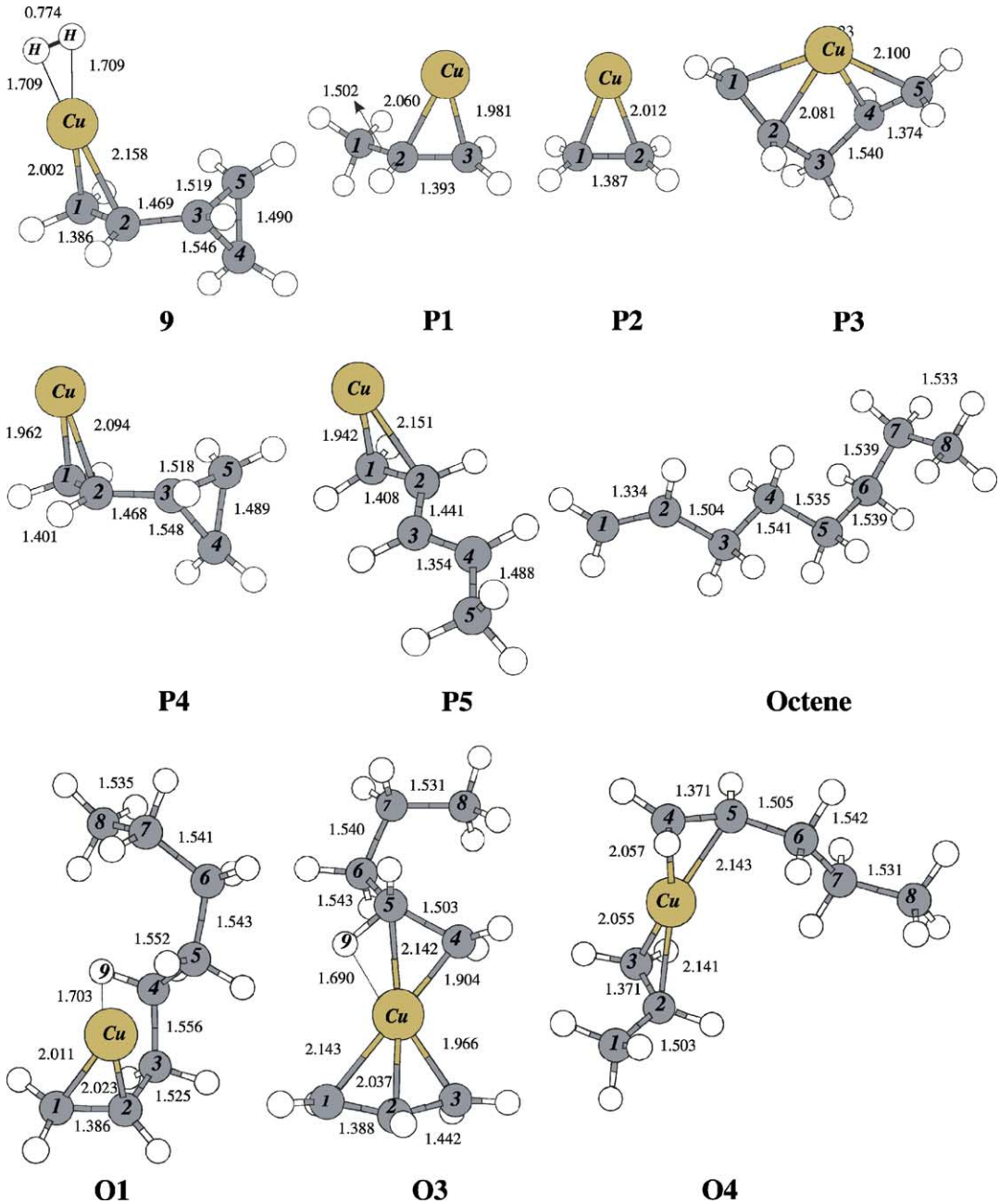

Fig. 2. (*Continued*).

be possible if the alkyl chain of 1-pentene in the corresponding Cu^+ complex was completely extended. Indeed, as shown in Fig. 2, there is a direct interaction between one of the γ-hydrogen atoms of the terminal methyl group and the metal. A second-order NBO analysis [45] shows that these interactions, named as agostic [47], involve a dative bond from the σ_{CH} bonding orbital to an empty orbital of the metal cation

Table 1
Total energies (E, hartrees), zero point energies (ZPE, hartrees) and relative energies (ΔE, kcal mol^{-1}) of the stationary points of the 1-pentene–Cu^+ and 1-octene–Cu^+ potential energy surfaces and the products of their unimolecular decomposition

System	B3LYP/6-31G*		B3LYP/6-311+(2df,2p)	
	E	ZPE	E	ΔE
1-Pentene + Cu^+	−1836.635643	0.137833	−1836.781708	0.0
1	−1836.748856	0.139898	−1836.866471	−51.9
2	−1836.632706	0.133170	−1836.750222	+16.8
3	−1836.719288	0.136792	−1836.824637	−27.6
4	−1836.777975	0.136572	−1836.888939	−68.1
5	−1836.719549	0.132789	−1836.844263	−42.4
6	−1836.687803	0.137573	−1836.827775	−29.5
7	−1836.683971	0.137803	−1836.824930	−27.1
8	−1836.691820	0.137641	−1836.828471	−29.5
9	−1836.701313	0.132800	−1836.828391	−32.5
TS13	−1836.704461	0.137103	−1836.813726	−20.6
TS34	−1836.703428	0.133445	−1836.810101	−20.5
P1	−1758.111903	0.082334	−1758.208597	–
P2	−1718.786874	0.054031	−1718.869733	–
P3	−1835.522975	0.116076	−1835.642054	–
P4	−1835.499845	0.117265	−1835.622611	–
P5	−1835.523015	0.115771	−1835.649390	–
1-Octene + Cu^+	−1954.575571	0.224067	−1954.760094	0.0
O1	−1954.688905	0.225532	−1954.845770	−52.8
O3	−1954.663733	0.222627	−1954.808449	−31.2
O4	−1954.730562	0.222151	−1954.880397	−76.7
TSO1O3	−1954.649669	0.223085	−1954.798324	−24.6
TSO3O4	−1954.648892	0.219053	−1954.794624	−24.8
H_2	−1.17548238	0.010142	−1.18001281	–
1-Pentene	−196.5336284	0.137833	−196.6050134	–
1-Octene	−314.4735565	0.224067	−314.5833999	–
C_2H_4	−78.58745733	0.051220	−78.62098348	–
C_3H_6	−117.9075543	0.080067	−117.9534481	–
C_5H_8	−195.2977684	0.113877	−195.3707745	–
Cu^+	−1640.102015	0.000000	−1640.176694	–

and a back-donation from one of the lone-pairs of Cu toward the σ_{CH^*} antibonding orbital (see Table 2). As a consequence, the C5–H6 linkage becomes weaker and longer favoring the C–H cleavage on going from complex **1** to complex **2**, and also the evolution from complex **3** toward complex **4**. This weakening of the C–H bond is reflected in a large red-shifting (424 cm^{-1}) of the corresponding C–H stretching frequency (see Table 3) in the complex **1** compared to the free alkene. Also consistently, in complex **1** there is a bcp between Cu and this hydrogen atom of the terminal methyl group. Simultaneously, there is also a sizable charge donation from the C=C double bond to the metal and a back donation from the metal to the C–C π-antibonding molecular orbital (see Table 2). The result is a lengthening of the C=C bond whose stretching frequency appears shifted to the red by 142 cm^{-1} (see Table 3). Also consistently, two bcps are found between Cu and the two carbons of the C=C linkage, with a rather similar topology to that described before for $(C_2H_4)Cu^+$ complexes [48]. Hence, in complex **1** the metal cation is formally tri-coordinated. The electronic depletion undergone by the C=C double bond enhances the electronegativity of the carbon atoms, which accordingly polarize the rest of the alkyl chain whose C–C bonds also become slightly longer. A perusal of the C–C stretching frequencies in complex **1** shows that, indeed, all of

Table 2
Orbital interactions (kcal mol^{-1}) obtained by means of a NBO second-order perturbation analysis, for pentene–Cu$^+$ complexes

Complex	Dative interactions		Back-donation	
	Orbitals involved	Energy	Orbitals involved	Energy
1	π(C1–C2) → LP*(Cu)	61.5	LP(Cu) → π*(C1–C2)	28.6
	σ(C5–H6) → LP*(Cu)	19.0	LP(Cu) → σ*(C5–H6)	5.9
2	π(C1–C2) → LP*(Cu)	42.5	LP(Cu) → π*(C1–C2)	43.2
3	π(C1–C2) → LP*(Cu)	51.5	LP(Cu) → π*(C1–C2)	8.5
	σ(C2–C3) → LP*(Cu)	10.5	LP(Cu) → σ*(C2–C3)	2.0
	σ(C3–C4) → LP*(Cu)	147.0	LP(Cu) → σ*(C3–C4)	69.1
	σ(C4–C5) → LP*(Cu)	11.8	LP(Cu) → σ*(C4–C5)	2.5
	σ(C5–H6) → LP*(Cu)	31.4	LP(Cu) → σ*(C5–H6)	11.0
4	π(C2–C3) → LP*(Cu)	84.6	LP(Cu) → π*(C3–C3)	20.2
	π(C4–C5) → LP*(Cu)	80.3	LP(Cu) → π*(C5–C10)	23.6

them appear slightly shifted to the red with respect to the neutral 1-pentene molecule (see Table 3).

Once the adduct **1** has been formed, the dissociative attachment mechanism involves, as a first step, a hydrogen shift from the terminal methyl group toward Cu. This leads to a significant weakening of the C3–C4 bond concomitant with the formation of ethene. Quite interestingly the first step in the pseudo-insertion mechanism (**1** → **3**) involves the same bond weakening, but without hydrogen shift. Why this second process is thermodynamically favored while the first one is not, is the next question that has to be answered. In both processes, **1** → **2** and **1** → **3** there is a reinforcement of both, the C2–C3 bond within one of the moieties interacting with Cu$^+$ and the C4–C5 bond within the other moiety. There are however two other factors that contribute to destabilize complex **2** with respect to complex **3**. Firstly, that in the former we have changed a strong C–H bond by a much weaker Cu–H linkage. Secondly, the formation of this new Cu–H bond prevents an effective interaction of the metal with the ethylene moiety, so that while in complex **3** Cu is hexa-coordinated in complex **2** it is only tri-coordinated. Indeed, a NBO second-order perturbation analysis shows (see Table 2) that in complex **2** there is a normal Cu–H chemical bond and a dative bond from the π(C1=C2) bonding orbital toward an empty (formally the 4s) orbital of Cu and a back donation from a lone-pair of Cu toward the π*(C1=C2) antibonding orbital. This implies that in complex **2**, the metal is formally tri-coordinated and coherently one Cu–H and two Cu–C bcps can be located in this structure, with charge densities of 0.118 and 0.090 e au^{-3}, respectively. The bonding pattern of complex **3** is much more complicated. As shown in Table 2, the strongest interaction involves a dative

Table 3
Harmonic vibrational frequencies (cm^{-1}) of pentene and pentene–Cu$^+$ complexes

System	Bond				
	C–H[a]	C1–C2	C2–C3	C3–C4	C4–C5
Pentene	3043	1731	1186	1069[b]	856[b]
1	2619	1589	1164	1040	854
2	1938[c]	1591	938	258	1337
3	2338	1582	1223	560; 497[d]	1040
4	3053	911	1351	376	1320

[a] Stretching frequency of one of the C–H bonds of the methyl group, the one that in complexes **1** and **3** interacts with the metal cation.

[b] These two values correspond to the asymmetric and symmetric combinations, respectively, of the C3–C4 and C4–C5 stretching modes.

[c] This value corresponds to the new Cu–H bond formed in this complex.

[d] The C3–C4 stretching in this complex appear replaced by the asymmetric and the symmetric combinations of the C3–Cu–C4 stretching.

bond from the σ(C3–C4) bonding orbital to an empty orbital of Cu, and a strong back-donation from a lone-pair of Cu toward the σ*(C3–C4) antibonding orbital. This effect is so strong that, in complex **3**, the C3–C4 bond appears practically broken, with a charge density at the bcp (0.142 e au^{-3}) much smaller than that typically found in conventional C–C bonds. Concomitantly, a bcp with a charge density of 0.105 e au^{-3} is found between Cu and C3, and another one, with a charge density of 0.121 e au^{-3}, between Cu and C4. Similar bonding and back-bonding interactions are found involving the C1=C2, the C2–C3, the C4=C5 and the C5–H6 bonds (see Table 2), confirming that in this structure Cu is formally hexa-coordinated. This bonding pattern is also mirrored in the set of stretching vibrational frequencies. As illustrated in Table 3, on going from complex **1** to complex **3**, the C1=C2 appears slightly shifted to the red as well as the C5–H6. Conversely, the C2–C3 and the C4–C5 stretching frequencies appear blue-shifted, and the C3–C4 stretch appear replaced by the asymmetric and the symmetric combination of the C3–Cu and Cu–C4 stretching displacements.

A subsequent transfer of one of the hydrogen atoms of the methyl group of the H_2C–CH_3 moiety of complex **3** toward the H_2C–CH=CH_2 one, through the transition state **TS34**, stabilizes the system significantly. It is worth noting that the existence of the aforementioned agostic interaction between Cu and the hydrogen of the methyl group favors this migration and as a consequence the **3** → **4** process implies a low (7 kcal mol^{-1}) activation barrier.

Once complex **4** is formed, two different unimolecular dissociation processes, into C_2H_4 + [H_3C–CH=CH_2–Cu]$^+$ (**P1**) and into C_2H_6 + [H_2C=CH_2–Cu]$^+$ (**P2**) are possible. Taking into account that, as it could be anticipated, the calculated binding energy of Cu$^+$ to H_3C–CH=CH_2 is larger than that to H_2C=CH_2, the first exit channel is thermodynamically favored, in nice agreement with the experimental evidence. In fact, complex **4**, Cu is formally tetracoordinated, but as shown in Table 2, the dative bond from the C2=C3 bond is stronger than that involving the C4=C5 linkage, reflecting the inductive effect of the methyl group.

4.1.2. Routes for dehydrogenation

As indicated in preceding sections, a minor fragmentation of 1-pentene–Cu$^+$ corresponds to the loss of H_2. One possible mechanism would involve the formation of complex **5** as a precursor for this loss. However, although this complex is quite stable, it should be formed reasonably by a second hydrogen shift from complex **2**. This implies that such a mechanism should be discarded, because, as we have already mentioned above, the formation of complex **2** is an endothermic process.

Alternative pathways for the loss of H_2 can be envisaged as the result of attachment of Cu$^+$ to the methylene or the methyl groups of 1-pentene, namely complexes **6**–**8**. All attempts to find complexes in which Cu$^+$ forms a five-membered ring by association with the C3–H and C4–H bonds failed, because all these structures collapsed to different conformers of complex **1**, depending on the relative conformation of the alkyl chain (see Scheme 2).

As explained in [47], the agostic-type interactions in complexes **6**–**8** can be viewed as three-center-*n*-electron bonds between a d orbital of Cu and the s orbitals of the two hydrogen atoms involved in the bonding (see Scheme 3).

The main consequence is that the C–H bonds become weaker, and therefore, lengthen significantly. More importantly, these complexes are found to be much more stable than complex **2**, and therefore, they can play a significant role in the observed loss of H_2. Several mechanisms can now be envisaged with origin in these complexes. Among them we have considered that (named as **III** in Fig. 1) with origin in complex **8**, because it can be a precursor of complex **9**, which would eventually dissociate by loosing a H_2 molecule yielding complex **P4**, that easily isomerizes to yield a more stable complex **P5**, in which the cyclopropane ring evolved to yield a HC=CH–CH_3 moiety. It is worth mentioning that all attempts to directly produce complex **P5** through an activation of the allylic alpha C–H bond failed, because all the initial structures envisaged collapsed to complex **8**, from which only complex **9** can be formed.

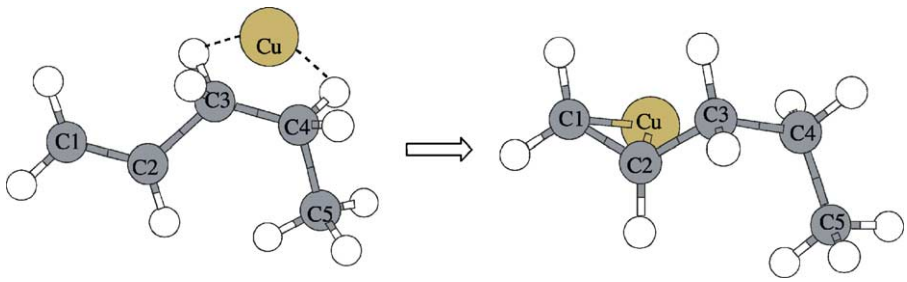

Scheme 2.

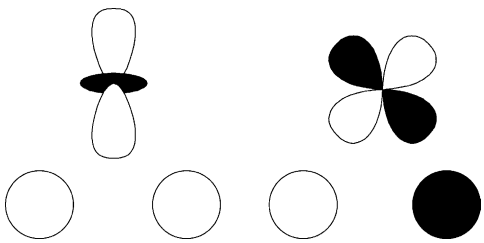

Scheme 3.

4.2. 1-Octene + Cu^+ reactions

As already mentioned, the MIKE spectrum of 1-octene–Cu^+ complex is dominated by the loss of C_3H_6 (100%), whereas the loss of C_5H_{10} (6%) corresponds to a much less intense fragmentation. The selectivity of these reactions, which have been discussed in the case of 1-pentene–Cu^+ complex is clearly revealed by the data given in Table 4. We can see, for example, that the 1,1-d_2-1-octene–Cu^+ complex eliminates specifically $C_3H_4D_2$, and that the 6,6-d_2, 7,7-d_2 and 8,8,8-d_3-1-octene–Cu^+ complexes lose exclusively C_3H_6. On the other hand, the losses of deuterated pentene, which are the counterpart of the major fragmentation, occur also without scrambling.

These last experimental results seem to indicate that the hydrogen transfer that leads to the C_3H_6 elimination is *specific* and consequently, the hydrogen atom involved in this mechanism is the γ-hydrogen atom. No doubt, conclusive experiments would require the use of C5 deuterated species. Unfortunately, several attempts to synthesize this labeled compound failed. However, in the light of the aforementioned results and the theoretical calculations carried out for 1-octene–Cu^+ reactions (vide infra), we can safely conclude that only the γ-hydrogen atom plays a role, and therefore, α and β positions can be reasonably discarded.

Concerning the H_2 elimination, the MIKE spectra of labeled compounds (8,8,8-d_3-1-octene, the 7,7-d_2-1-octene and the 6,6-d_2-1-octene) show that the corresponding signals are extremely weak or even absent. This weak dehydrogenation could be an artifact of the MIKE scan but it should be noted that this

Table 4
Principal fragmentations observed in the MIKE spectra of ^{65}Cu adducts of 1-octene isotopologues[a]

	Neutral losses				
	C_3H_6	$C_3H_4D_2$	C_5H_{10}	$C_5H_8D_2$	$C_5H_7D_3$
1-Octene	100		6		
1,1-d_2-1-Octene		100			
6,6-d_2-1-Octene	100			5	
7,7-d_2-1-Octene	100			5	
8,8,8-d_3-1-Octene	100				5

[a] Intensities are given in percentages of the base peak.

reaction was also observed in CAD spectra already reported by Peake and Gross [27].

In this theoretical section, for the sake of conciseness, we shall analyze only the so-called pseudo-insertion mechanism **II**. The relative stabilities of the stationary points of the PES along this mechanism have been also included in Fig. 1. These values clearly show that mechanism **II** is again consistent with the experimental evidence. As it was found for 1-pentene, the whole PES lies below the entrance channel, and the overall processes leading to $[C_5H_{10}Cu]^+$ and $[C_3H_6Cu]^+$ complexes are clearly exothermic. It is also worth noting that the main bonding characteristics of the complexes involved resemble closely those already discussed for 1-pentene. For example, the most stable conformation of the 1-octene–Cu^+ adduct corresponds to a π-complex (**O1**) in which the alkyl chain is folded to enhance its interaction with the metal cation (see Fig. 2). As expected, the binding energy for 1-octene is 1.9 kcal/mol larger than for 1-pentene. Also, the equivalent structure to complex **3**, namely **O3**, was found to be a local minimum of the octene–Cu^+ PES, the only difference being again its relative stability with respect to complex **O1**. These two local minima are connected through a transition state, **TSO1O3**, which, as in the case of 1-pentene–Cu^+ reactions, involves a C3–C4 bond cleavage. Finally, a subsequent hydrogen shift, through the transition state **TSO3O4**, in which Cu acts as a carrier would leads to complex **O4**, again equivalent to complex **4** in the 1-pentene–Cu^+ PES.

In summary, our calculations show that the PES for the pseudo-insertion mechanism in 1-octene–Cu^+ and 1-pentene–Cu^+ processes are rather similar, even though the whole PES for 1-octene–Cu^+ is slightly shifted to lower energies with respect to the 1-pentene–Cu^+ PES, mainly due to the expected enhanced interaction between 1-octene and Cu^+. The second important difference between 1-pentene and 1-octene is that, in the latter case, once the **O4** complex is formed, the most favorable unimolecular fragmentation corresponds to the loss of C_3H_6, which in the case of 1-pentene was the minor product. Essentially, however, there are no basic reactivity differences between both systems because the unimolecular dissociation of complexes **4** and **O4** is governed by the relative binding energies to Cu^+ of the two moieties forming the complex. In other words, in both cases the smaller fragment (C_2H_4 or C_3H_6, respectively) is the one preferably lost, because due to its smaller polarizability binds the metal cation less strongly. Hence, we can safely conclude that no significant changes should be observed in the topology of the PES for different R substituents. So, for 1-hexene and 1-heptene (R = CH_3 and C_2H_5, respectively) one should expect, as for 1-octene, C_3H_6 to be the main dissociation product, in good agreement with the experimental evidence [19].

5. Conclusions

The topology of the PES associated with 1-pentene–Cu^+ reactions confirms the pseudo-insertion mechanism tentatively proposed by Fordham et al. [19], is the most favorable one. In this mechanism, the attachment of the metal cation to the π-system forces a coiling of the alkyl chain which favors the formation of an hexa-coordinated intermediate much more stable than the complexes formed along a typical dissociative attachment process. In both mechanisms the agostic interactions between the metal cation and the C–H bonds of the alkene play an important role. We have also shown that the main features of the pseudo-insertion mechanism, implies the γ-hydrogen atom and do not change when the alkyl chain attached to the C=C double bond is much longer, as in the case of 1-octene. Hence, we can safely conclude that this mechanism would explain in general the specific reactivity of Cu^+ with 1-alkenes containing five or more carbon atoms, representing a reliable analytical method to determine the position of the double bond.

We have also shown that the loss of H_2 systematically observed in these gas-phase processes, could be related with the ability of Cu^+ to yield strong agostic interactions either with the methylene groups or with the terminal methyl group of the alkyl chain.

Acknowledgements

This work has been partially supported by the DGI Project No. BQU2000-0245, by the Acción Integrada Picasso HF-2001-0042 and by the NATO Grant SA CRG 973140. A generous allocation of computational time at the CCC of the Universidad Autónoma de Madrid is also gratefully acknowledged.

References

[1] K. Eller, H. Schwarz, Chem. Rev. 91 (1991) 1121.
[2] B.S. Freiser (Ed.), Organometallic Ion Chemistry, Kluwer Academic Publishers, Dordrecht, 1995.
[3] P.B. Armentrout, Ann. Rev. Phys. Chem. 52 (2001) 423.
[4] A. Fontijn (Ed.), Gas-Phase Metal Reactions, North Holland, Amsterdam, 1992.
[5] S. Yano, M. Otsuka (Eds.), Marcel Dekker, New York, 1996.
[6] A. Sigel, H. Sigel (Eds.), Metal Ions in Biological Systems, Marcel Dekker, New York, 1996.
[7] S.H. Niu, M.B. Chem. Rev. 100 (2000) 353.
[8] P.E.M. Siegbahn, R.A. Blomberg, Chem. Rev. 100 (2000) 421.
[9] M. Torrent, M. Solà, G. Frenking, Chem. Rev. 100 (2000) 439.
[10] E.R. Davidson, Chem. Rev. 100 (2000).
[11] M. Alcamí, O. Mo, M. Yanez, Mass Spectrom. Rev. 20 (2001) 195.
[12] D. Schröder, S. Shaik, H. Schwarz, Acc. Chem. Res. 33 (2000) 139.
[13] S. Bärsch, D. Schröder, H. Schwarz, Int. J. Mass Spectrom. 202 (2000) 363.
[14] S. Bärsch, D. Schröder, H. Schwarz, P.B. Armentrout, J. Phys. Chem. A 105 (2001) 2005.
[15] A.R. Dongré, V.H. Wysocki, Org. Mass Spectrom. (1994) 700.
[16] E.M. Sible, S.P. Brimmer, J.A. Leary, J. Am. Soc. Mass Spectrom. (1997) 32.
[17] S.P. Gaucher, J.A. Leary, Anal. Chem. 70 (1998) 3009.
[18] J.P. Morizur, B. Desmazieres, J. Chamot-Rooke, V. Haldys, P. Fordham, J. Tortajada, J. Am. Soc. Mass Spectrom. 9 (1998) 731.
[19] P.J. Fordham, J. Chamot-Rooke, E. Giudice, J. Tortajada, J.P. Morizur, J. Mass Spectrom. 34 (1999) 1007.
[20] T.M. Sack, M.L. Gross, Anal. Chem. 55 (1983) 2419.
[21] D.A. Peake, M.L. Gross, D.P. Ridge, J. Am. Chem. Soc. 106 (1984) 4307.
[22] D.A. Peake, M.L. Gross, Anal. Chem. 57 (1985) 115.
[23] T.M. Sack, M.L. Gross, Anal. Chem. 57 (1985) 1290.
[24] D.A. Peake, S.-K. Huang, M.L. Gross, Anal. Chem. 59 (1987) 1557.
[25] M.L. Gross, Adv. Mass Spectrom. 11A (1989) 792.
[26] M.L. Gross, Mass Spectrom. Rev. 8 (1989) 186.
[27] D.A. Peake, M.L. Gross, J. Am. Chem. Soc. 109 (1987) 600.
[28] P.B. Armentrout, J.L. Beauchamp, L.F. Halle, J. Am. Chem. Soc. 103 (1981) 6624.
[29] H. Schwarz, D. Schroeder, Pure Appl. Chem. 72 (2000) 2319.
[30] R.B. Freas, J.E. Campana, J. Am. Chem. Soc. 107 (1985) 6202.
[31] A.M. Duffield, R. Beugelmans, H. Budzikiewicz, D.A. Lightner, D.H. Williams, C. Djerassi, J. Am. Chem. Soc. 87 (1965) 805.
[32] J.-P. Morizur, C. Djerassi, Org. Mass Spectrom. 5 (1971) 895.
[33] M.J. Frisch, G.W. Trucks, H.B. Schlegel, G.E. Scuseria, M.A. Robb, J.R. Cheeseman, V.G. Zakrzewski, J.J.A. Montgomery, R.E. Stratmann, J.C. Burant, S. Dapprich, J.M. Millam, A.D. Daniels, K.N. Kudin, M.C. Strain, O. Farkas, J. Tomasi, V. Barone, M. Cossi, R. Cammi, B. Mennucci, C. Pomelli, C. Adamo, S. Clifford, J. Ochterski, G.A. Petersson, P.Y. Ayala, Q. Cui, K. Morokuma, D.K. Malick, A.D. Rabuck, K. Raghavachari, J.B. Foresman, J. Cioslowski, J.V. Ortiz, B.B. Stefanov, G. Liu, A. Liashenko, P. Piskorz, I. Komaromi, R. Gomperts, R.L. Martin, D.J. Fox, T. Keith, M.A. Al-Laham, C.Y. Peng, A. Nanayakkara, C. Gonzalez, M. Challacombe, P.M.W. Gill, B. Johnson, W. Chen, M.W. Wong, J.L. Andres, C. Gonzalez, M. Head-Gordon, E.S. Replogle, J.A. Pople, Gaussian 98, revised A3. Gaussian, Inc. 1999.
[34] A.D. Becke, J. Chem. Phys. 98 (1993) 5648.
[35] C. Lee, W. Yang, R.G. Parr, Phys. Rev. B: Condens. Matter 37 (1988) 785.
[36] A.J.H. Watchers, J. Chem. Phys. 52 (1970) 1033.
[37] P.J. Hay, J. Chem. Phys. 66 (1977) 4377.
[38] C.W. Bauschlicher, Chem. Phys. Lett. 246 (1995) 40.
[39] T. Ziegler, Chem. Rev. 91 (1991) 651.
[40] A. Luna, M. Alcami, O. Mo, M. Yanez, Chem. Phys. Lett. 320 (2000) 129.
[41] A. Luna, B. Amekraz, J. Tortajada, Chem. Phys. Lett. 266 (1997) 31.
[42] B.J. Lynch, D.G. Truhlar, Chem. Phys. Lett. 361 (2002) 251.
[43] R.F.W. Bader, Atoms in Molecules. A Quantum Theory, Clarendon Press, Oxford, 1990.
[44] R.F.W. Bader, J.R. Cheeseman, AIMPAC Program, 2000.
[45] A.E. Reed, L.A. Curtiss, F. Weinhold, Chem. Rev. 88 (1988) 899.
[46] F. Weinhold, NBO Program 5.0. University of Wisconsin System, 2001.
[47] I. Corral, O. Mó, M. Yáñez, Int. J. Mass Spectrom. 227 (2003) 401.
[48] R.H. Hertwig, W. Koch, D. Schroeder, H. Schwarz, J. Hrusak, P. Schwerdtfeger, J. Phys. Chem. 100 (1996) 12253.